Photochemistry and Photobiology, 2006, 82: 1385–1390

Rapid Communication

Light-Driven Water Splitting for (Bio-)Hydrogen Production: Photosystem 2 as the Central Part of a Bioelectrochemical Device

Adrian Badura[1], Berndt Esper[1], Kenichi Ataka[2], Christian Grunwald[3], Christof Wöll[3], Jürgen Kuhlmann[4], Joachim Heberle[2,5] and Matthias Rögner*[1]

[1]Plant Biochemistry, Faculty of Biology, Ruhr-University Bochum, D-44780 Bochum, Germany
[2]Forschungszentrum Jülich, IBI-2: Structural Biology, D-52425 Jülich, Germany
[3]Physical Chemistry I, Faculty of Chemistry, Ruhr-University Bochum, D-44780 Bochum, Germany
[4]Max Planck Institute of Molecular Physiology, Dortmund, Germany
[5]Biophysical Chemistry, University Bielefeld, D-33615 Bielefeld, Germany

Received 14 July 2006; accepted 28 July 2006; published online 9 August 2006 DOI: 10.1562/2006-07-14-RC-969

ABSTRACT

To establish a semiartificial device for (bio-)hydrogen production utilizing photosynthetic water oxidation, we report on the immobilization of a Photosystem 2 on electrode surfaces. For this purpose, an isolated Photosystem 2 with a genetically introduced His tag from the cyanobacterium *Thermosynechococcus elongatus* was attached onto gold electrodes modified with thiolates bearing terminal Ni(II)-nitrilotriacetic acid groups. Surface enhanced infrared absorption spectroscopy showed the binding kinetics of Photosystem 2, whereas surface plasmon resonance measurements allowed the amount of protein adsorbed to be quantified. On the basis of these data, the surface coverage was calculated to be 0.29 pmol protein cm^{-2}, which is in agreement with the formation of a monomolecular film on the electrode surface. Upon illumination, the generation of a photocurrent was observed with current densities of up to 14 μA cm^{-2}. This photocurrent is clearly dependent on light quality showing an action spectrum similar to an isolated Photosystem 2. The achieved current densities are equivalent to the highest reported oxygen evolution activities in solution under comparable conditions.

INTRODUCTION

Hydrogen is one of the most promising energy carriers among environmentally friendly and clean energy sources for the future. For this reason, alternative strategies for its production must be developed because most hydrogen is still produced from fossil fuels, which involves environmental pollution (1). One strategy is to use natural systems as blueprint for either the design of appropriately modified natural systems or for the construction of semiartificial or fully artificial model systems. Among the energy converting processes in nature, light-driven water splitting photosynthesis of microalgae and higher plants is the key process. If the extremely effective photosynthetic energy conversion could be efficiently combined with the biological process of hydrogen production via the enzyme hydrogenase, this would represent a significant step toward the development of environmentally acceptable, regenerative systems for (bio-)hydrogen production.

Because optimizing the efficient combination of both processes (*i.e.* photosynthesis and hydrogen production) in a living cell is still a long-term process, which is especially hampered by the extreme oxygen sensitivity of almost all hydrogenases, the electrochemical connection of the involved redox enzymes—Photosystem 2 (PS2), Photosystem 1 (PS1) and hydrogenases—within a photochemical cell, converting light energy into hydrogen, now appears more promising. Although various versions of such photochemical devices have already been proposed in the past (2–6), several recently determined crystal structures of the three principal redox enzymes (7–11) enable a completely new approach to this topic: They contribute considerably to a mechanistic understanding of the involved electron transfer processes and allow—in combination with genetic engineering tools—their directed modification.

Realization of a semiartificial system for biohydrogen production involves the integration of photosynthetic protein complexes and hydrogenases into a bioelectronic or bioelectrochemical device. Practically, this can be achieved by the immobilization of the protein complexes on conductive supports (*e.g.* noble-metals, carbon or semiconductors), in which the first step is the efficient electron transfer from light-driven water splitting by PS2 to the conductive surface.

A possible arrangement of photosynthetic proteins and hydrogenases is depicted in Fig. 1. PS2 complexes immobilized on the anodic part of the photochemical cell transfer electrons for the reduction of immobilized PS1 on the cathode, which in turn, can supply electrons for the catalytic reduction of protons by the coimmobilized or linked hydrogenase. The energy required to overcome the potential difference between water oxidation and proton reduction is supplied by the light-induced processes of the two photosystems.

Successful steps toward a functional cathodic part (*i.e.* hydrogen production *via* immobilized hydrogenases on electrodes), have

*Corresponding author email: matthias.roegner@ruhr-uni-bochum.de (Matthias Rögner)

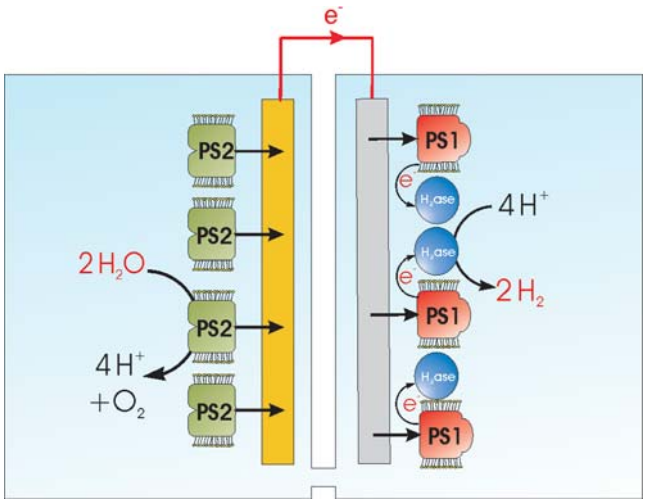

Figure 1. Proposed model of a semiartificial system for biohydrogen production based on immobilized PS2/PS1 complexes and hydrogenases.

already been reported by various groups (12–17); they show convincingly the remarkable catalytic properties of hydrogenase modified electrodes toward proton reduction. Electrochemical studies could also indicate how to exploit the photocatalytic properties of PS1 complexes (18–20). The combination of those or an advanced cathodic part with a functional and efficient anodic part consisting of PS2 immobilized on an electrode surface would be a further valuable contribution toward a clean production of hydrogen according to the model of Fig. 1.

Here we report on an optimized PS2 immobilization strategy on gold surfaces that is, from our point of view, the central part within such a device and decisive for its efficiency. We present an efficient method to achieve current densities, which are up to ~1200 times higher than those obtained in previous works (21,22).

Our approach is based on a simple and common immobilization method using His-tagged PS2 on thiolated gold surfaces. As shown in previous studies (23–25), such a recombinant protein allows a reversible binding *via* metal affinity interactions to exposed Ni(II)-nitrilotriacetic acid (NTA) groups on the gold surface. Qualitatively, this binding to the surface was monitored by surface enhanced infrared absorption spectroscopy (SEIRAS), whereas the surface coverage was determined by surface plasmon resonance (SPR) spectroscopy. Using these results, we could establish an optimized light dependent electrochemical communication between PS2 and a gold electrode with activities corresponding to the highest oxygen-evolving rates achieved in solution.

MATERIALS AND METHODS

Biochemical preparations. CP43-His-tagged PS2 was prepared from mass cultures of *Thermosynechococcus elongatus* in a 20 L photobiofermenter as reported Kuhl *et al.* (26). Solubilized membrane proteins were purified by immobilized metal ion affinity chromatography (Chelating Sepharose, Amersham Biosciences AB, Uppsala, Sweden) as a first chromatographic step using the affinity of the genetically introduced His-tag of PS2 to the Ni(II)-NTA matrix of the column. The elution of PS2 was induced by a linear gradient up to 100 m*M* L-histidine in the buffer solution (20 m*M* 2-(N-morpholino)-ethane sulphonic acid [MES], 10 m*M* $MgCl_2$, 10 m*M* $CaCl_2$, 300 m*M* NaCl and 0.03 % [w/v] n-dodecyl-β-D-maltoside [β-DM, Biomol]). After dialysis in 20 m*M* MES, 10 m*M* $MgCl_2$, 10 m*M* $CaCl_2$ and 0.03 % (w/v) β-DM isolated complexes were further purified by ion exchange chromatography (Uno-Q6 column, Bio-Rad Laboratories, Germany) yielding an active dimeric subpopulation of PS2 complexes with a typical oxygen evolution activity of 4000–6000 μmol O_2 (mg chlorophyll [Chl])$^{-1}$ h^{-1}. Samples were stored in buffer containing 0.5 *M* mannitol at 1–2 mg Chl mL^{-1} at –70°C prior to use.

Surface modification. Prior to the immobilization of His-tag PS2 complexes, a self-assembled monolayer was deposited on the respective surface by immersing the gold substrate in a dimethyl-sulfoxide (DMSO) solution of 10 m*M* 1-octanethiol (Sigma-Aldrich, Germany) and 0.1 m*M* 16-mercaptohexadecanoic acid (Sigma-Aldrich) for 1 h. After removal from the solution the surface was rinsed several times with DMSO and finally dried under a nitrogen stream. To activate the carboxy-groups of 16-mercaptohexadecanoic acid, the modified surface was kept in a solution of 10 m*M* N-hydroxysuccinimide (Sigma-Aldrich) and 10 m*M* 1-ethyl-3-[3-(dimethylamino)propyl]carbodiimide (Sigma-Aldrich) was diluted in ultrapure water (Seralpur Pro 90 CN, Seral) for 1 h and rinsed thereafter with water to remove unreacted species. Binding of the NTA group was induced by incubation of the surface in 150 m*M* Nα′,Nα$^{\bullet}$″-bis(carboxymethyl)-L-lysine (Fluka, Switzerland), dissolved in 0.5 *M* K_2CO_3 buffer, pH = 9.8, for 90 min, followed by washing with water. For the complexation of Ni^{2+} ions, the surface was kept in 100 m*M* $NiSO_4$ for 30 min and finally rinsed with water.

Spectroscopy. For the SEIRAS experiments, a gold film was deposited on the flat surface of a single reflexion silicon hemicylindrical prism (20 mm width × 25 mm height × 10 mm radius) by an electroless deposition technique (27). The adsorption process of PS2 onto the modified surface was monitored starting with 1 mg mL^{-1} His-tagged PS2 in buffer solution (20 m*M* MES, 10 m*M* $MgCl_2$, 10 m*M* $CaCl_2$ and 0.03 % [w/v] β-DM). Unbound PS2 complexes were removed by washing with buffer.

For the SPR spectroscopic measurements, first an adhesive sublayer (10 nm) of titanium was evaporated on the surface of a 10 × 10 mm glass substrate followed by a 100 nm layer of gold (28) After priming the surface with buffer solution (see above), the kinetics of PS2 adsorption were monitored in a Biacore 1000 (Biacore, Uppsala Sweden) flow system at a flow rate of 5 μL min^{-1}. For the desorption of PS2 complexes, the Ni(II)-NTA surface was flushed with buffer solution containing 200 m*M* L-histidine.

Bioelectrochemical investigations. For electrochemical measurements, a three-electrode system was used consisting of a Pt-counter electrode, a gold disc working electrode (∅ = 2 mm, CH-Instruments, USA) and an Ag/AgCl reference electrode (WPI, USA) with 3 *M* KCl as electrolyte. The amperometric measurements were performed with an AUTOLAB PGSTAT 12 potentiostat (Metrohm, Switzerland).

Prior to the experiments, the working gold electrode was cleaned by polishing with 0.3 μm aluminum oxide paste (LEKO) and rinsed thereafter several times with water. Recording of a cyclovoltammogram in 1 *M* KOH was used to check the cleanness of the surface. After the surface modification (see above), PS2 complexes were immobilized by incubation of the gold electrode in 0.25 mg mL^{-1} buffered protein solution (see above) for 1 h in the dark. To remove unspecifically bound PS2 complexes from the surface the gold electrodes were incubated in buffer solution for 10 min in the dark. The procedure was repeated twice with fresh buffer.

Electrochemical experiments with immobilized PS2 complexes were carried out at 30°C in buffered electrolyte containing 1 m*M* 2,6-dichloro-1,4-benzoquinone (Sigma-Aldrich) as the electron acceptor for PS2. Response from immobilized PS2 was registered by applying an oxidation potential of 0.3 V for 2,6-dichloro-1,4-benzoquinone (DCBQ) and recording the time dependence of the current. Immobilized PS2 was illuminated with a halogen cold light reflexion lamp using a 675 nm interference filter (Schott, Germany) and a cold light filter Calflex 3000 (Balzers, Liechtenstein) to protect the sample from excessive heat.

Cyclic voltammetry was performed with 50 μ*M* 2,6-dichloro-1,4-benzoquinone at a scan rate of 1 mV s^{-1} between –0.04 V and +0.34 V vs. Ag/AgCl.

Action spectra were recorded with interference filters and filter combinations, respectively, between 405 nm and 737 nm (Schott).

RESULTS AND DISCUSSION

Surface modification

The integration of photosynthetic proteins into a bioelectrochemical device requires a targeted structuring of the surface in order to

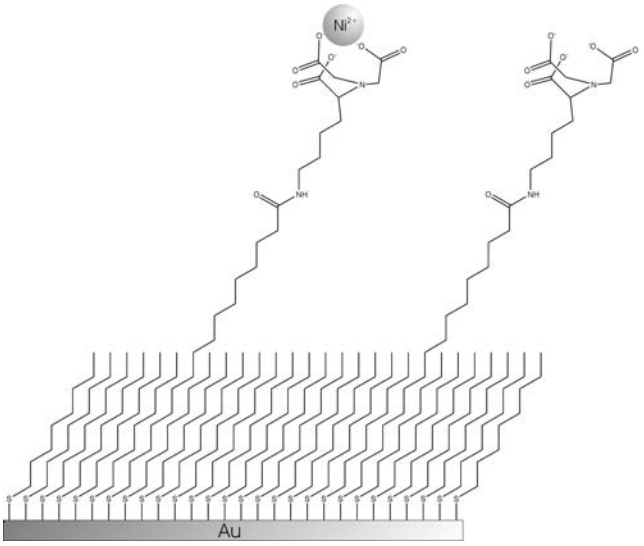

Figure 2. Scheme for surface structuring on a gold surface with mixed thiolates (*i.e.* 1-octanethiol and 16-mercaptohexadecanoic acid [MHA]). The carboxy group of MHA was activated with NHS/EDC for binding of ANTA, which forms a complex with Ni^{2+} ions.

achieve a well controlled and preferably reversible attachment of the enzymes. By using appropriately ω-functionalized organothiol self-assembled monolayers (SAMs), an organic surface with predefined composition and properties can be generated. To immobilize His-tagged PS2 *via* metal ion affinity interaction with Ni(II)-NTA groups, we chose carboxyalkylthiolates; this allowed us to anchor the amino-terminated NTA moiety by forming an amide bond (activation was carried out using NHS/EDC (*N*-hydroxysuccinimide/1-ethyl-3-[3-(dimethylamino)propyl]carbodiimide) (29). The density of COOH groups on the surface was controlled by diluting 16-mercaptohexadecanoic acid (MHA) with 1-octanethiol (1-OT). An MHA:1-OT ratio of 1:100 was found to yield the highest surface coverage of specifically bound protein molecules.

Figure 2 shows the modified MHA/1-OT SAM surface after treatment with EDC/NHS and amino-nitrilotriacetic acid (ANTA). Each of the surface modification steps was monitored by SEIRAS (data not shown; see Ataka *et al.* for a similar strategy, 23).

Qualitative analysis by SEIRAS

SEIRAS measurements were performed to verify and monitor the adsorption process of detergent-solubilized dimeric PS2 complexes onto the Ni(II)-NTA/1-OT modified surface (see above); for comparison, a reference spectrum was recorded in buffer solution. Upon addition of solubilized PS2 complexes, bands appear at 1659, 1545 and around 1400 cm^{-1} (Fig. 3a), with the former two bands representing the amide I and II modes of the PS2-protein backbone vibrations, respectively. The increase of the band intensities reflects the accumulation of PS2 on the Ni(II)-NTA surface. Although the bands around 1400 cm^{-1} could not be clearly assigned, they may originate from Ni(II)-NTA as suggested by Ataka *et al*. (23). Figure 3b shows the binding kinetics of the His-tagged PS2 complexes to the Ni(II)-NTA as obtained by plotting the intensity of the amide I band as a function of the adsorption time. Exponential and linear fitting (continuous line) yields a time constant of $\tau = 294\ s^{-1}$, however, without reaching saturation,

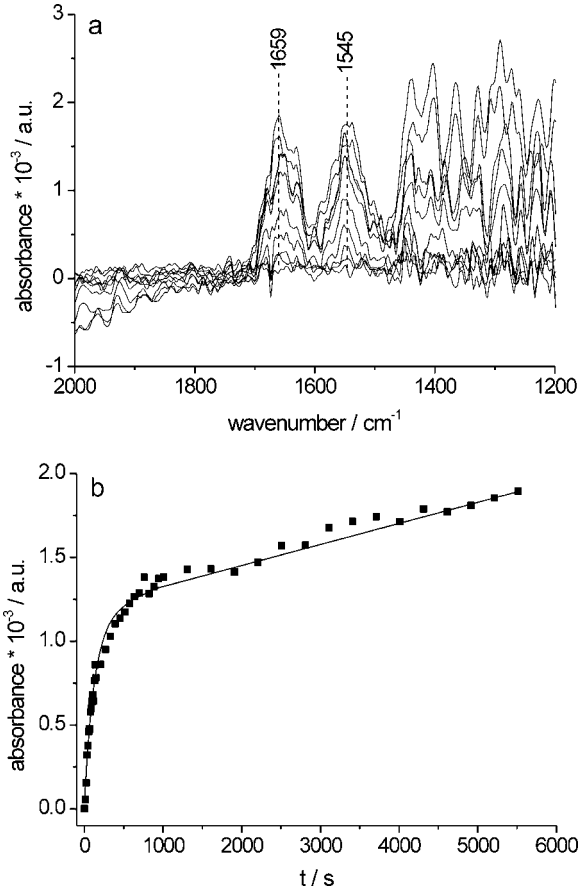

Figure 3. (a) SEIRA spectra of His-tagged PS2 adsorbed to the Ni(II)-NTA SAM modified gold surface *via* metal ion affinity. PS2 complexes were added to a final concentration of 1 mg × mL^{-1}. Absorbance increase of the bands indicates the binding of the protein to the surface. (b) Adsorption kinetics of PS2 onto the Ni(II)-NTA SAM/Au modified surface. The peak height of the amide I band at 1659 cm^{-1} was plotted versus the adsorption time. The continuous line represents the fit of an exponential and a linear term.

which is due to a baseline drift during the measurement time of 90 min.

Quantitative analysis by SPR

Although SEIRAS is very useful for the qualitative analysis of adsorption processes of molecules on surfaces, it is rather difficult to determine the surface coverage of immobilized PS2. This can be achieved by the SPR technique, which can monitor the adsorption of PS2 complexes on the modified surface under continuous flow conditions as shown in Fig. 4.

After pretreatment of the surface with buffer the detergent-solubilized protein (0.25 mg mL^{-1}) was injected resulting in a signal increase due to both the rapid change in refractive index between the buffer and the protein solution (bulk effect) and association of PS2 complexes. On reinjection of buffer a fast decrease in the SPR signal could be observed (reverse bulk effect) followed by a slower decay showing the dissociation of protein from the surface. The amount of PS2 bound specifically to the surface was tested by washing with buffer containing 200 m*M* L-histidine. Injection of 200 m*M* His resulted in a strong bulk signal due to the different refractive indices of the two buffers. Desorption of specifically bound PS2 can be

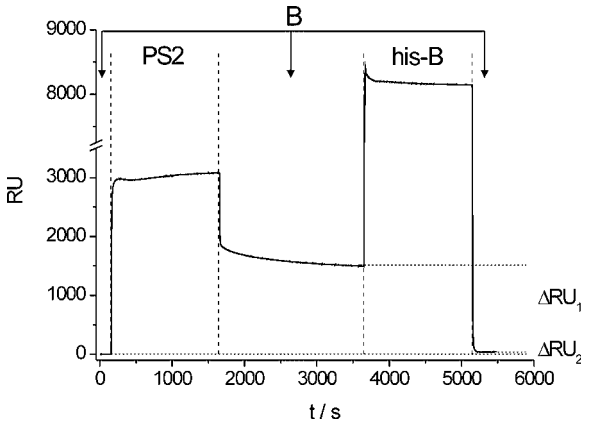

Figure 4. SPR signal on binding of His-tagged PS2 onto a Ni(II)-NTA SAM modified gold surface, followed by dissociation of the protein with 200 m*M* L-histidine. Characters on top of the figure represent the individual steps of the surface treatment: B = washing with buffer, PS2 = association of His-tagged PS2 complexes and his-B = washing with buffer containing 200 m*M* L-histidine. ΔRU_1 = specifically bound fraction of the protein, ΔRU_2 = unspecifically bound fraction. For further details see the text.

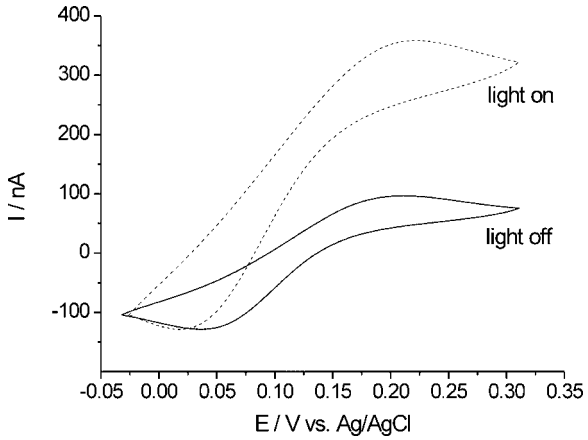

Figure 5. Cyclic voltammetry of DCBQ (50 μ*M*) with His-tag PS2 immobilized on the surface of a Ni(II)-NTA SAM functionalized gold disc working electrode (∅ = 2 mm); the potential range is –0.04 V to +0.34 V (vs. Ag/AgCl) at a scan rate of 1 mV s^{-1}. Supporting electrolyte was a buffer solution with 20 m*M* MES pH 6.5, 10 m*M* $MgCl_2$, 10 m*M* $CaCl_2$, 0.03% (w/v) β-DM. The voltammetric scan was performed under illumination (100 μmol photons m^{-2} s^{-1} at 675 nm, dashed line), or in darkness (continuous line).

observed after the end of the treatment with histidine because His replaces the PS2 complexes from the Ni(II)-NTA coordination site. The difference between the resonance units (RU) before and after the last washing step corresponds to the fraction of putatively specific bound PS2 accounting for ∅ ΔRU_1 = 1458 RU (±59 RU), corresponding to averaged data from three measurements. The baseline elevation between the start and end levels corresponds to unspecifically bound PS2 (*e.g.* denaturated protein) accounting for ∅ ΔRU_2 = 63 RU (±26 RU) (see Fig. 4). Assuming a molecular mass of ~500,000 g mol^{-1} for dimeric PS2 (26) and considering that 1 RU corresponds to 1 pg protein mm^{-2} (Biacore manual, www.biacore.com) the surface coverage of specifically bound PS2 is 0.29 pmol cm^{-2}, whereas the unspecifically bound part remaining after the His washing amounts to 0.01 pmol cm^{-2}. With dimensions of 20.5 × 11.0 nm for dimeric PS2 complexes (7), which are extended by a detergent layer of about 3 nm, a maximum coverage of ~0.37 pmol PS2 cm^{-2} can be estimated. This corresponds to a specific coverage of ~78% and an unspecific surface coverage of ~2%, which is in agreement with a monolayer of PS2 complexes attached to the Ni(II)-NTA groups *via* His tag.

Bioelectrochemical investigations

For the establishment of an efficient bioelectrochemical device, the communication between the immobilized enzyme and the electrode surface is crucial. We therefore generated the same thiol-based Ni(II)-NTA surfaces as reported above on gold disc electrodes (∅ = 2 mm). Due to the long distance, direct electron transfer between the electrode and PS2 complexes is inefficient (30) and artificial electron mediators are required. Among the tested soluble redox components interacting with the Q_B binding site of PS2, DCBQ was most suitable according to oxygen evolution/producing measurements.

Figure 5 shows the cyclic voltammogram of a PS2 modified electrode. The first cycle was performed without light showing a typical cyclovoltammogram of DCBQ with redox waves indicating the oxidation at +0.2 V and the reduction at +0.04 V, respectively. Upon illumination a strong increase of anodic current was observed in the same potential range as where DCBQ oxidation occurs. Without PS2 such a response was not observed (*i.e.* excitation of PS2 leads to the catalytic reduction of DCBQ at the Q_B site and approximation of its oxidation potential during the potential scan is the reason for the anodic current increase). This clearly demonstrates the electrochemical communication between PS2 complexes and the electrode as mediated by DCBQ.

Figure 6 shows the response of the electrode upon illumination of immobilized PS2 in a chronoamperometric experiment applying a potential of +0.3 V to oxidize DCBQ.

Immobilized PS2 was excited with red light of 675 nm at an intensity of ~100 μmol photons m^{-2} s^{-1} for 5 s. During this light pulse the strong signal remained stable, while it decreased rapidly to the baseline upon switching off the light. The average current density was about 14 μA cm^{-2}.

The surface coverage determined by SPR measurement (see above) can be converted into the nonflow bioelectrochemical approach because here too, several washing steps were applied to remove loosely bound PS2 after the immobilization (*i.e.* a similar amount of adsorbed protein molecules can be expected). Based on the surface coverage of 1.74×10^{11} dimeric PS2 complexes (0.29 pmol cm^{-2}), this is equivalent to the transfer of 502 electrons per second (ET = 1.4 10^{-5} A/[1602 10^{-19} As * 1.74 10^{11}]) or 125 O_2 released per second and dimeric complex by water splitting. Because each PS2 dimer contains 70 Chl (31), an oxygen evolution rate of 6430 O_2 Chl^{-1} h^{-1} (*e.g.* $oxygen_{evolution}$ = 125 O_2 s^{-1} * [3600/70]) can be calculated, corresponding to a turnover rate of ~4 ms per reaction center. This estimated oxygen evolution rate is equivalent to the highest published rate achieved with isolated PS2 particles (26); interestingly, they have been prepared from WT cells of the same cyanobacterium using a similar procedure. Also, the calculated turnover rates are in agreement with previously proposed values for PS2 (32). This indicates that there is no loss in activity due to the immobilization procedure.

The immobilization of PS2 has been realized earlier, but so far the reported approaches suffer from rather low photocurrent densities (21,22). The current densities determined in our setup are ~1200 times higher than those published by Maly *et al.* (21) (0.0113 μA cm^{-2}) in a similar approach. The authors calculated an

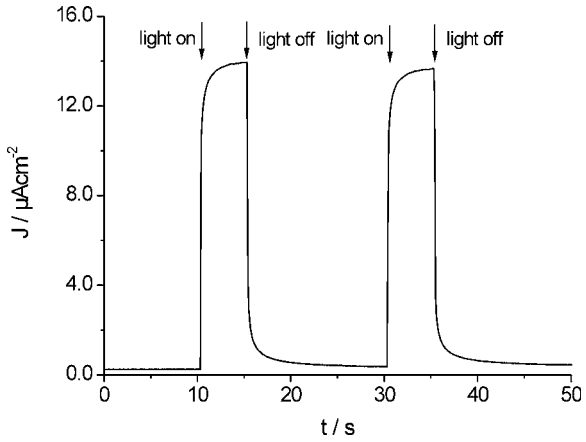

Figure 6. Current response upon illumination of immobilized His-tag PS2 on the surface of a Ni(II)-NTA SAM functionalized gold disc working electrode (∅ = 2 mm). The applied potential was +0.3 V vs. Ag/AgCl. As supporting electrolyte, a buffer solution containing 20 m*M* MES pH 6.5, 10 m*M* $MgCl_2$, 10 m*M* $CaCl_2$, 0.03 % (w/v) β-DM was used; 1 m*M* DCBQ was added as electron acceptor. The modified working electrode was illuminated with 100 µmol photons m^{-2} s^{-1} at 675 nm.

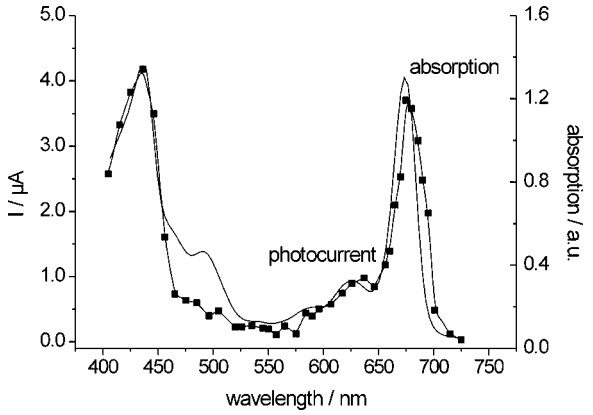

Figure 7. Action spectrum of immobilized His-tag PS2. Wavelength dependence of the generated photocurrent was determined between 405 and 725 nm in steps of 5–10 nm (black squares). Generated photocurrents were normalized to the interference filter transmission and the lamp spectrum. For comparison, the absorption spectrum of isolated PS2 complexes in solution is also shown (full line).

approximately four times higher surface coverage of PS2 (1.18 pmol cm^{-2}), which clearly indicates the presence of a multilayer film of adsorbed PS2 based on a theoretical value of 0.37 pmol cm^{-2} for the maximum coverage. These results suggest that PS2 was mainly adsorbed unspecifically, because apart from the Ni(II)-NTA groups, amino terminated thiolates were also used, which show strong proteophilic properties (33). The combination of these effects certainly retards the diffusion of the electron mediator to the electrode, causing the low current densities upon illumination of the immobilized PS2.

In contrast, the extremely high current densities in our study result from the applied immobilization strategy: It prevented the diffusion retardation of the reduced electron mediator to the electrode surface by a too densely packed protein layer and consequently allowed an efficient electron transfer. To this end, the optimal choice of the electron mediator—DCBQ—might also have contributed.

Action spectrum of the photocurrent

The photocurrent of PS2 immobilized on the electrode surface was investigated to determine its dependence on the light quality. The resulting action spectrum is shown in Fig. 7 in comparison with the absorption spectrum of PS2 in solution. Both spectra agree perfectly with the highest current around the absorption maxima at 430 nm and 675 nm, respectively. Also, this current could be inhibited by specific inhibitors of PS2 acting at the Q_B site of the D1 subunit, such as Atracine, DCMU (3-[3,4-dichlorophenyl]-1,1-dimethyl-urea), Phenmedipham (3-methoxycarbonylaminophenyl-[3′methyl-phenyl]-carbamate) or Dinoterb (2-terbutyl-4,6-dinitrophenol) (results not shown).

In summary, these results further confirm that the generated photocurrent is due to the mediated electron transfer from immobilized PS2 complexes *via* DCBQ to the gold electrode.

CONCLUSION

Here we presented a simple and cost-efficient procedure (all reagents are commercially available) for the integration of PS2 complexes into a bioelectrochemical device, which is considered as decisive step toward a semiartificial (bio-)hydrogen production. Mixed thiols of 1-octanethiol and 16-mercaptohexadecanoic acid could efficiently be introduced to immobilize dimeric PS2 complexes on a gold surface *via* Ni(II)-NTA (bound to the latter compound), which allowed a specific and reversible attachment of the protein to the surface. The adsorption process as monitored by SEIRAS and SPR technique revealed that specific binding of the detergent-solubilized PS2 to the surface achieved almost 80% of the theoretically predicted surface coverage, whereas the non-specific binding was minimized successfully down to 2%.

Amperometric experiments showed an efficient mediated electron transfer between immobilized PS2 complexes and the electrode, with current densities corresponding to the highest oxygen evolution rates measured with isolated PS2 complexes to date. Such a high yield of PS2 activity is most probably due to the high stability of the thermophilic PS2 preparation, combined with an individual immobilization method for PS2. This is in contrast to all other immobilization procedures reported up to now that apparently used excess PS2, making aggregation and multilayer formation unavoidable.

The improvement achieved for PS2 in this report is an excellent basis for further optimizing the efficiency and the long-term stability, for instance, of PS2-based bioelectrochemical devices. The final goal is the realization of a model device (34) that integrates both photosynthetic proteins and hydrogenases (see Fig. 1) and transports electrons from the water splitting site of PS2 on the anode *via* immobilized PS1 on the cathode to the hydrogenase, which catalyzes the reduction of protons to hydrogen. If successful, such a model photochemical cell could be the blueprint for the future development of an environmentally acceptable, regenerative system for (bio-)hydrogen production.

Acknowledgements—This work was supported by the DFG (SFB 480, Project C1, and European Graduate College 795 to M.R.), by the European Union (SOLAR-H to M.R.) and VW Stiftung (to J.H.). R. Oworah-Nkruma and C. Koenig are acknowledged for the excellent technical assistance. We thank A. Trebst and W. Schuhmann (Ruhr-University Bochum) for valuable discussions.

REFERENCES

1. Kruse, O., J. Rupprecht, J. H. Mussgnug, G. C. Dismukes and B. Hankamer (2005) Photosynthesis: A blueprint for solar energy capture and biohydrogen production technologies. *Photochem. Photobiol. Sci.* **4**, 957–970.
2. Grätzel, M. (2001) Photoelectrochemical cells. *Nature* **414**, 338–344.
3. Haehnel, W. and H. J. Hochheimer (1979) On the current generated by a galvanic cell driven by photosynthetic electron transport. *J. Electroanal. Chem.* **104**, 563–574.
4. LaVan, D. A. and J. N. Cha (2006) Approaches for biological and biomimetic energy conversion. *Proc. Natl. Acad. Sci. U S A* **103**, 5251–5255.
5. Lewis, N. S. (2001) Light work with water. *Nature* **414**, 589–590.
6. Wenk, S.-O., D. J. Qian, T. Wakayama, C. Nakamura, N. Zorin, M. Rögner and J. Miyake (2002) Biomolecular device for photoinduced hydrogen production. *Int. J. Hydrogen Energy* **27**, 1489–1493.
7. Ferreira, K. N., T. M. Iverson, K. Maghlaoui, J. Barber and S. Iwata (2004) Architecture of the photosynthetic oxygen-evolving center. *Science* **303**, 1831–1838.
8. Jordan, P., P. Fromme, H. T. Witt, O. Klukas, W. Saenger and N. Krauss (2001) Three-dimensional structure of cyanobacterial photosystem I at 2.5 A resolution. *Nature* **411**, 909–917.
9. Nicolet, Y., C. Piras, P. Legrand, C. E. Hatchikian and J. C. Fontecilla-Camps (1999) Desulfovibrio desulfuricans iron hydrogenase: The structure shows unusual coordination to an active site Fe binuclear center. *Structure* **7**, 13–23.
10. Peters, J. W., W. N. Lanzilotta, B. J. Lemon and L. C. Seefeldt (1998) X-ray crystal structure of the Fe-only hydrogenase (cpi) from *Clostridium pasteurianum* to 1.8 angstrom resolution. *Science* **282**, 1853–1858.
11. Zouni, A., H. T. Witt, J. Kern, P. Fromme, N. Krauss, W. Saenger and P. Orth (2001) Crystal structure of photosystem II from *Synechococcus elongatus* at 3.8 A resolution. *Nature* **409**, 739–743.
12. Lamle, S. E., K. A. Vincent, M. Halliwell, S. P. Albracht and F. A. Armstrong (2003) Hydrogenase on an electrode: A remarkable heterogeneous catalyst. *Dalton Trans.* **21,** 4152–4157.
13. Leger, C., A. K. Jones, W. Roseboom, S. P. Albracht and F. A. Armstrong (2002) Enzyme electrokinetics: Hydrogen evolution and oxidation by allochromatium vinosum [nife]-hydrogenase. *Biochemistry* **41**, 15736–15746.
14. Pershad, H. R., J. L. Duff, H. A. Heering, E. C. Duin, S. P. Albracht and F. A. Armstrong (1999) Catalytic electron transport in chromatium vinosum [nife]-hydrogenase: Application of voltammetry in detecting redox-active centers and establishing that hydrogen oxidation is very fast even at potentials close to the reversible H+/H2 value. *Biochemistry* **38**, 8992–8999.
15. Qian, D. J., C. Nakamura, S. O. Wenk, H. Ishikawa, N. Zorin and J. Miyake (2002) A hydrogen biosensor made of clay, poly(butylviologen), and hydrogenase sandwiched on a glass carbon electrode. *Biosens. Bioelectron.* **17**, 789–796.
16. Rudiger, O., J. M. Abad, E. C. Hatchikian, V. M. Fernandez and A. L. De Lacey (2005) Oriented immobilization of desulfovibrio gigas hydrogenase onto carbon electrodes by covalent bonds for non-mediated oxidation of H2. *J. Am. Chem. Soc.* **127**, 16008–16009.
17. Tye, J. W., M. B. Hall and M. Y. Darensbourg (2005) Better than platinum? Fuel cells energized by enzymes. *Proc. Natl. Acad. Sci. U S A* **102**, 16911–16912.
18. Das, R., P. J. Kiley, M. Segal, J. Norville, A. A. Yu, L. Wang, A. S. Trammell, L. E. Reddick, R. Kumar, F. Stellacci, N. Lebedev, J. Schnur, B. D. Bruce, S. Zhang and M. Baldo (2004) Integration of photosynthetic protein molecular complexes in solid-state electronic devices. *Nano Lett.* **4**, 1079–1083.
19. Millsaps, J. F., B. D. Bruce, J. W. Lee and E. Greenbaum (2001) Nanoscale photosynthesis: Photocatalytic production of hydrogen by platinized photosystem I reaction centers. *Photochem. Photobiol.* **73**, 630–635.
20. Proux-Delrouyre, V., C. Demaille, W. Leibl, P. Setif, H. Bottin and C. Bourdillon (2003) Electrocatalytic investigation of light-induced electron transfer between cytochrome C6 and photosystem I. *J. Am. Chem. Soc.* **125**, 13686–13692.
21. Maly, J., J. Krejci, M. Ilie, L. Jakubka, J. Masojidek, R. Pilloton, K. Sameh, P. Steffan, Z. Stryhal and M. Sugiura (2005) Monolayers of photosystem II on gold electrodes with enhanced sensor response—Effect of porosity and protein layer arrangement. *Anal. Bioanal. Chem.* **381**, 1558–1567.
22. Maly, J., J. Masojidek, A. Masci, M. Ilie, E. Cianci, V. Foglietti, W. Vastarella and R. Pilloton (2005) Direct mediatorless electron transport between the monolayer of photosystem II and poly(mercapto-p-benzoquinone) modified gold electrode—New design of biosensor for herbicide detection. *Biosens. Bioelectron.* **21**, 923–932.
23. Ataka, K., F. Giess, W. Knoll, R. Naumann, S. Haber-Pohlmeier, B. Richter and J. Heberle (2004) Oriented attachment and membrane reconstitution of His-tagged cytochrome C oxidase to a gold electrode: In situ monitoring by surface-enhanced infrared absorption spectroscopy. *J. Am. Chem. Soc.* **126**, 16199–16206.
24. Sigal, G. B., C. Bamdad, A. Barberis, J. Strominger and G. M. Whitesides (1996) A self-assembled monolayer for the binding and study of histidine-tagged proteins by surface plasmon resonance. *Anal. Chem.* **68**, 490–497.
25. Tinazli, A., J. Tang, R. Valiokas, S. Picuric, S. Lata, J. Piehler, B. Liedberg and R. Tampe (2005) High-affinity chelator thiols for switchable and oriented immobilization of histidine-tagged proteins: A generic platform for protein chip technologies. *Chemistry* **11**, 5249–5259.
26. Kuhl, H., J. Kruip, A. Seidler, A. Krieger-Liszkay, M. Bunker, D. Bald, A. J. Scheidig and M. Rogner (2000) Towards structural determination of the water-splitting enzyme. Purification, crystallization, and preliminary crystallographic studies of photosystem II from a thermophilic cyanobacterium. *J. Biol. Chem.* **275**, 20652–20659.
27. Ataka, K. and J. Heberle (2004) Functional vibrational spectroscopy of a cytochrome C monolayer: SEIDAS probes the interaction with different surface-modified electrodes. *J. Am. Chem. Soc.* **126**, 9445–9457.
28. Zybin, A., C. Grunwald, V. M. Mirsky, J. Kuhlmann, O. S. Wolfbeis and K. Niemax (2005) Double-wavelength technique for surface plasmon resonance measurements: Basic concept and applications for single sensors and two-dimensional sensor arrays. *Anal. Chem.* **77**, 2393–2399.
29. Lee, J. K., Y. G. Kim, Y. S. Chi, W. S. Yun and I. S. Choi (2004) Grafting nitrilotriacetic groups onto carboxylic acid-terminated self-assembled monolayers on gold surfaces for immobilization of histidine-tagged proteins. *J. Phys. Chem. B* **108**, 7665–7673.
30. Itamar Willner, E. K. (2000) Integration of layered redox proteins and conductive supports for bioelectronic applications. *Angew. Chem. Int. Ed.* **39**, 1180–1218.
31. Loll, B., J. Kern, A. Zouni, W. Saenger, J. Biesiadka and K. D. Irrgang (2005) The antenna system of photosystem II from *Thermosynechococcus elongatus* at 3.2 A resolution. *Photosynth. Res.* **86**, 175–184.
32. Barber, J. (2003) Photosystem II: The engine of life. *Q. Rev. Biophys.* **36**, 71–89.
33. Zimmermann, H., A. Lindgren, W. Schuhmann and L. Gorton (2000) Anisotropic orientation of horseradish peroxidase by reconstitution on a thiol-modified gold electrode. *Chemistry* **6**, 592–599.
34. Prodöhl, A., M. Ambill, E. El-Mohsnawy, J. Lax, M. Nowaczyk, R. Oworah-Nkruma, T. Volkmer, S.-O. Wenk and M. Rögner (2004) Modular device for hydrogen production: Optimization of (individual) components. In *Biohydrogen*, Vol. III (Edited by J. Mijake, Y. Igarashi and M. Roegner), pp. 171–179. Elsevier, Dordrecht, the Netherlands.